Abrasion of steel by ceramic coatings: Comparison of RF-DLC to sputtered B_4C

Stephen J. Harris[a], Gordon G. Krauss[a], Steven J. Simko[a], Timothy J. Potter[b], Robert W. Carpick[c], Bridget Welbes[c] and Martin Grischke[d]

[a] *Chemistry and Environmental Science Dept., MD 3083, Ford Research Labs, Dearborn MI 48121, USA*
[b] *Physics Dept., Ford Research Labs, Dearborn MI 48121, USA*
[c] *Engineering Physics Dept., University of Wisconsin, Madison, WI, USA*
[d] *Head, R&D Wear Protection, Balzers Ltd, P.O. Box 1000, FL-9496 Balzers, Liechtenstein*

Received October 28, 2001; accepted November 4, 2001

The abrasion rates of steel balls sliding against a very smooth diamond-like carbon (DLC) coating and a rough boron carbide (B_4C) coating are compared. The initial abrasiveness of the B_4C coating is about 2 orders of magnitude greater than that of the DLC coating. Both coatings exhibit a rapid decrease in their abrasiveness with sliding distance, but the details of the abrasion kinetics of these coatings are quite different. The abrasiveness of B_4C falls according to a simple power law, while the abrasiveness of the DLC remains constant for a duration that depends on the load and then switches rather suddenly to zero. An explanation for this different behavior is proposed. During the abrasion process the asperities on the B_4C are smoothed to a startling extent.

KEY WORDS: Abrasion; coating; DLC; B_4C; asperities.

1. Introduction

It has been proposed [1] that thin, hard ceramic coatings can act to protect components from rolling contact fatigue, in part by polishing asperities on their counterparts. These asperities are then no longer available to stress the coated part. In previous work we showed that the initial polishing ability or abrasiveness of sputtered ceramic films such as diamond-like carbon (DLC) [2] and boron carbide (B_4C) [3] correlates strongly with the coating hardness [4], just as is seen for ceramic powders [5]. We found that the rate at which the abrasiveness falls can be described with a remarkably simple power-law scaling relationship [6], and that the change in abrasiveness correlates with changes in the nanometer-scale—but not the micrometer-scale—morphology of the coating [2]. In order to more clearly understand the role played by the surface morphology of the coatings, we have examined and compared the abrasiveness of two systems: (1) a Si-containing DLC coating made in an RF plasma, which produces a very smooth surface finish; and (2) a relatively rough sputtered B_4C coating whose abrasion kinetics we have examined previously [3].

2. Experimental

The procedures for depositing the silicon-containing DLC [7] and the B_4C coating [3] have been described previously. The substrate was a carburized HRC 60 steel coupon polished to a surface finish of $Ra = 7\,nm$ (as measured with an optical profilometer). The intrinsic roughness of the DLC coating is much less than this value, so the Ra roughness of the coated coupon is the same as that of the uncoated coupon. The B_4C coating has a surface finish of $Ra = 400\,nm$ (optical profilometer), and it exhibits columnar growth, with the dominant surface features being the "caps" of these columns.

We used a ball-on-disk tribometer to slide 3.2 nm diameter 52100 steel balls against the disk at 10 cm/s for a range of loads in air. Under these unlubricated conditions, the calculated temperature rise at the B_4C asperities is on the order of 1° [8], which means that frictional heating plays no role. These temperature calculations are supported by the fact that the abrasion kinetics are unaffected by changes of up to an order of magnitude in the sliding speed. The worn surface of the ball was examined with an optical profilometer after wiping with ethanol to remove loose debris. Previously, we and others [9,10] estimated the volume of steel removed from the balls by using a geometric technique, measuring the diameter of the wear scar formed on the ball and assuming that the wear scar is perfectly circular and flat. This assumption is not always true, however, especially for small numbers of cycles. Therefore, we developed an improved technique to measure the volume removed, which involves numerically integrating the volume under the surface profile of the wear scar on the ball and subtracting that result from the volume of an unworn ball to calculate the missing volume [11].

1023-8883/02/0100-0043/0 © 2002 Plenum Publishing Corporation

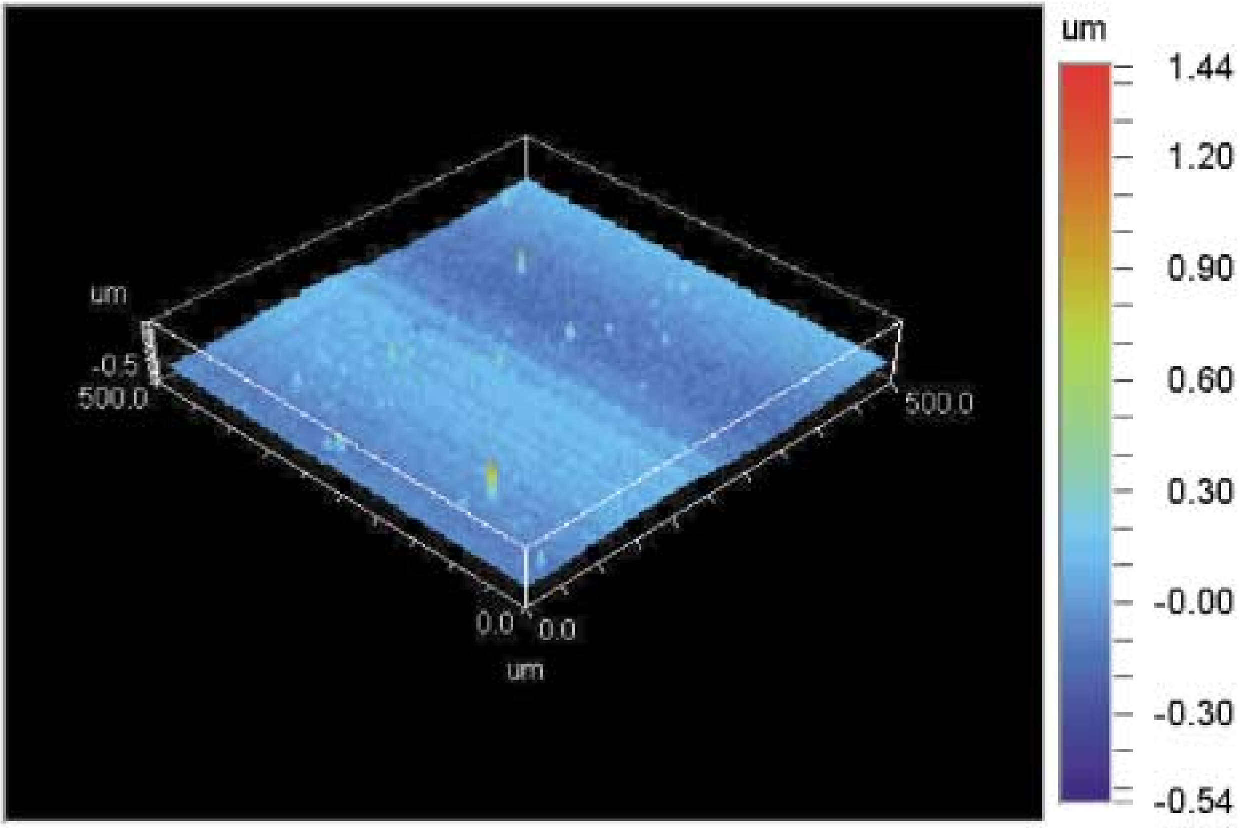

Figure 1. AFM image of a 500 × 500 μm region of the DLC coating.

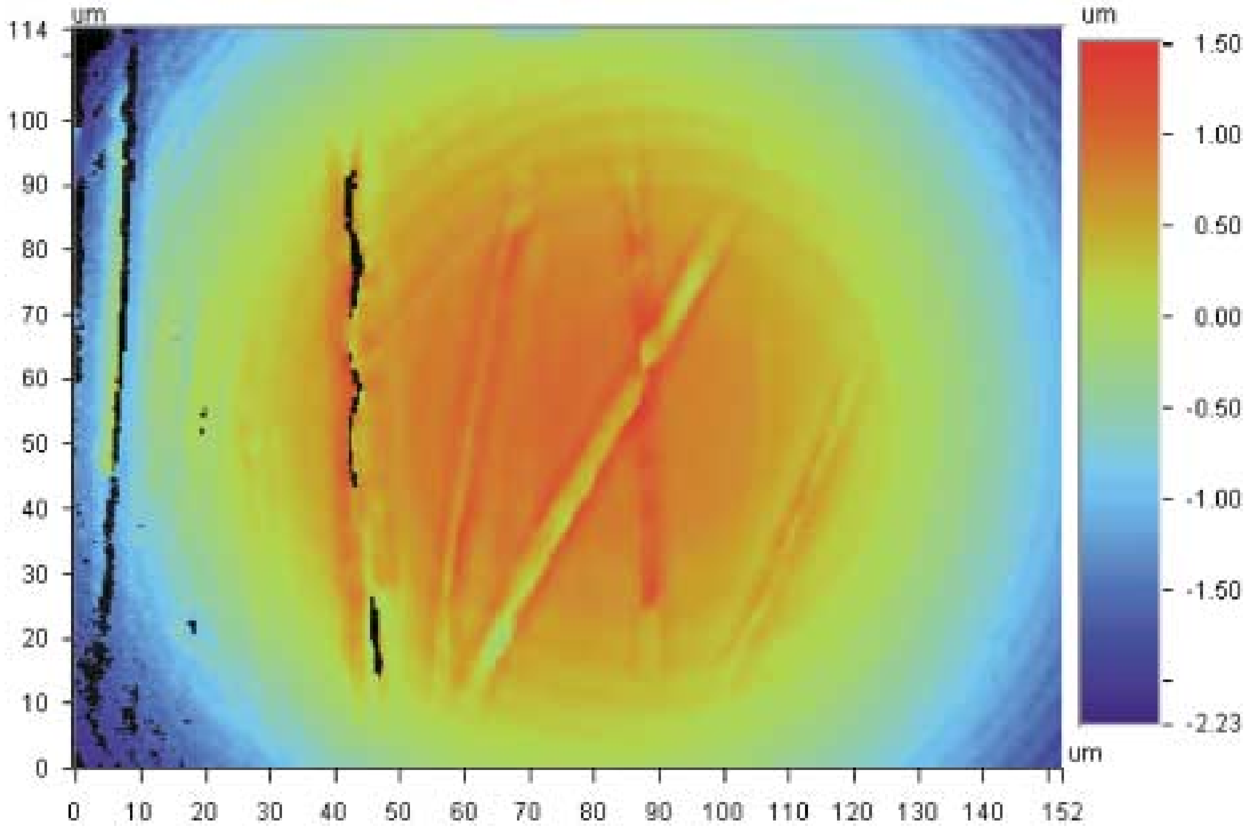

Figure 3. Optical profile of a steel ball after sliding for a distance of 1 mm.

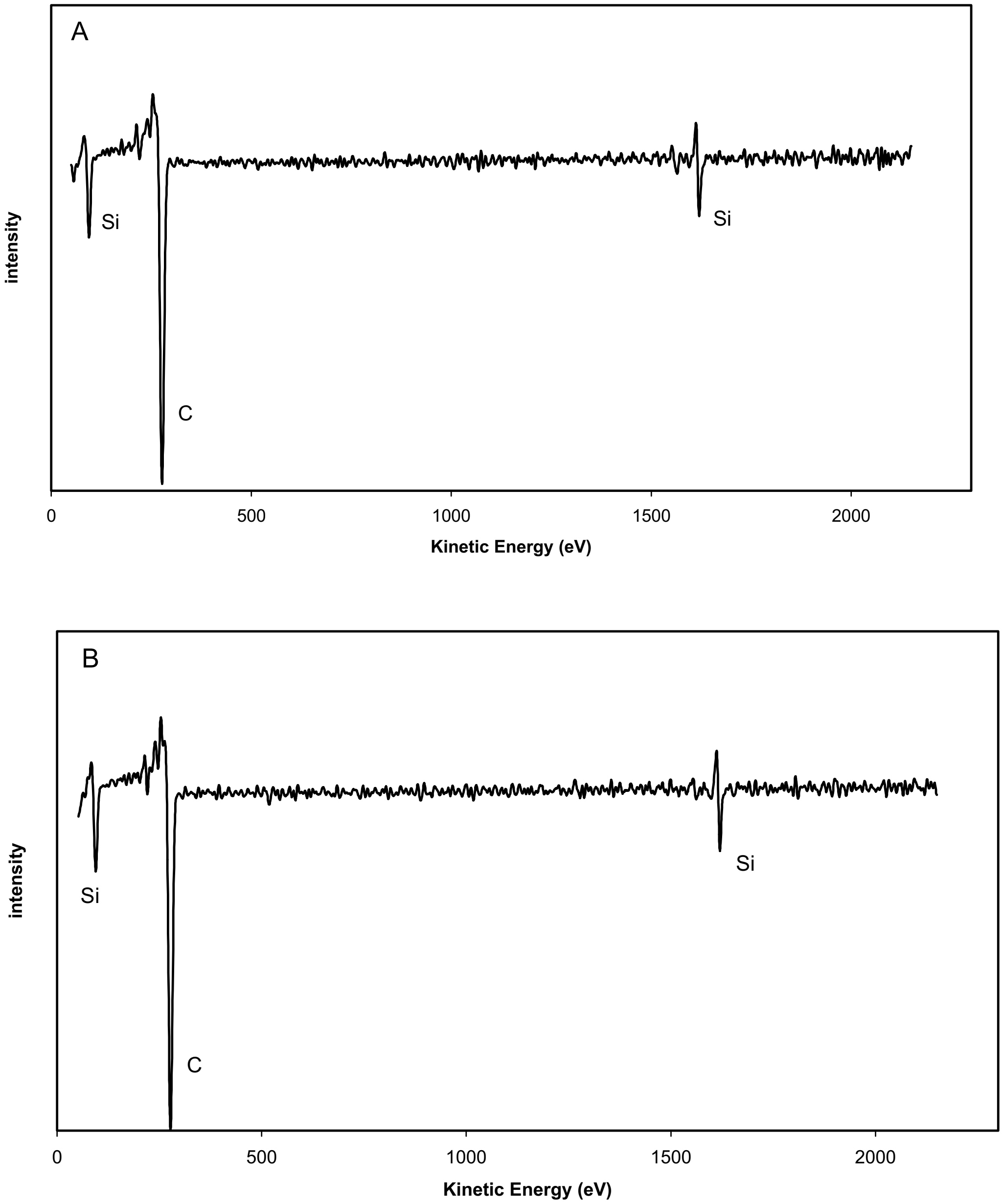

Figure 2. Auger electron spectra of an asperity (A) and the DLC coating (B) after 200 nm of sputtering, showing identical elemental compositions in these two regions.

This technique also has the advantage of being able to distinguish material removal from plastic deformation, both of which can cause scars on the ball.

Auger electron spectroscopy (AES) was used to examine the composition of asperities found on the surface of the DLC coating. (Auger analysis of the B_4C has been described previously). Data were acquired with a Physical Electronics model 680 scanning Auger microprobe employing a 10-kV, 10-nA primary electron beam.

Atomic force microscopy (AFM) images were acquired in contact mode under ambient conditions with a Digital Instruments Multimode AFM with a Nanoscope IIIA controller using silicon nitride tips, or with a Quesant Instruments Q-Scope 250 AFM using silicon tips. The AFM scanners used were independently calibrated with microfabricated spatial standards. AFM and profilometer image analysis was performed using Wyko Vision 32 software.

3. Results and discussion

3.1. DLC coating

Figure 1 shows an AFM image of the (unworn) DLC. The surface is mostly featureless apart from polishing marks on the steel substrate that are visible through the coating. However, a few asperities are also visible, the

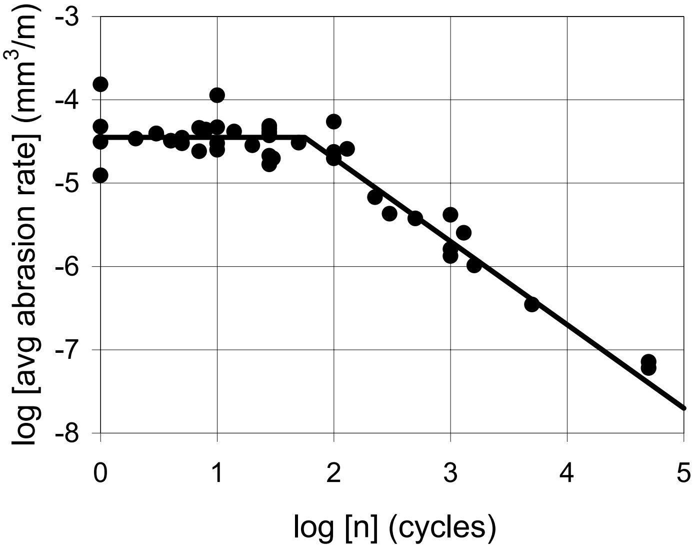

Figure 4. Abrasion kinetics for 1 Newton load. The solid line segments have slopes of 0 and −1.

tallest here being about 1.4 μm above the mean plane of the surface. Closer examination shows that each of these asperities covers an area of a few square microns. We generally find one or two such asperities, with heights typically ranging from around 0.1 to several μm, in any $100 \times 100\,\mu$m region, corresponding to 10^1–10^2/mm^2. This DLC surface is significantly different from the sort of surface generated by sputtering (see below). Since it is the asperities that cause the abrasion [12], we can expect very different abrasion kinetics.

The chemical identity of the material forming the asperities was determined using Auger spectroscopy. Figure 2 compares the chemical composition of the asperity to that of the bulk DLC film. Both regions show a mixture of carbon and silicon (~ 20 at%) which is indicative of a silicon-stabilized DLC film. Depth profiling results show that the composition remains constant to depths greater than 200 nm. The fact that nearly identical data were obtained in both areas suggests that these asperities are DLC particles that attach to the coating surface during the deposition.

Figure 3 is an optical profile of a ball which has slid against the DLC for a distance of just 1 mm. The width of the scratched region is about 0.1 mm, which means that the ball has contacted an area on the DLC about 0.1 mm wide $\times$ 1 mm long $=$ 0.1 mm^2. Given an asperity density of 10^1–10^2/mm^2, we expect that the ball should come into contact with about 1–10 asperities, making 1–10 grooves. This expectation is reasonably consistent with the image shown in figure 3.

Figure 4 shows a log–log plot of the average abrasion rate $\overline{A(n)}$ (total volume removed divided by total distance travelled) against n,

$$\overline{A(n)} \equiv \frac{V_{\text{total}}(n)}{2\pi r n} \qquad (1)$$

where $V_{\text{total}}(n)$ is the total volume removed during n cycles and r is the radius of the pin-on-disk track. For $n < 80$ the data are fit adequately with a line segment of slope zero at $\overline{A(n)} = 3 \times 10^{-5}\,\text{mm}^3/\text{m}$. According to equation (1), if $\overline{A(n)}$ is independent of n, then V_{total} is proportional to n, and the abrasion per meter is constant during those 80 cycles. Stated another way, since in this range the average abrasiveness does not change, then the instantaneous abrasiveness on the nth cycle A_{n} must be constant and equal to the average value, $\overline{A(n)}$. For $n > 80$ the data are fit adequately with a line whose slope is -1 and which passes through $\overline{A(n)} = 3 \times 10^{-5}$ at $n = 80$. According to equation (1) a slope of -1 means that V_{total} is constant; that is, abrasion has ceased. Thus, the good fit of the data to these two line segments indicates that the abrasiveness of the coating is constant for about 80 cycles and then, rather abruptly, goes to zero and stays there for at least tens of thousands of cycles. Figure 5(a) and (b) shows images of the scar on the steel ball at 100 and 10,000 cycles. The lack of significant material removal for $100 < n < 10{,}000$ is apparent.

Figure 6 shows abrasion kinetics data for 11 and 0.02 Newtons compared to the results for 1 Newton, which is shown as a heavy dashed line. In each case the data can be fit with a line segment of slope zero for low n and a slope -1 for higher n. At 0.02 Newtons the knee in the abrasiveness comes at around 250 cycles, while at 11 Newtons the break comes at around 40 cycles. However, above 250 cycles the average volume removed per meter is independent of the load between 0.02 to 11 Newtons, a range of a factor of 550. In effect, the three experiments show that the DLC can cause a certain total amount of material removal, and this can be extracted slowly, at 0.02 Newtons, or quickly, at 11 Newtons. The asperities causing this abrasion are either

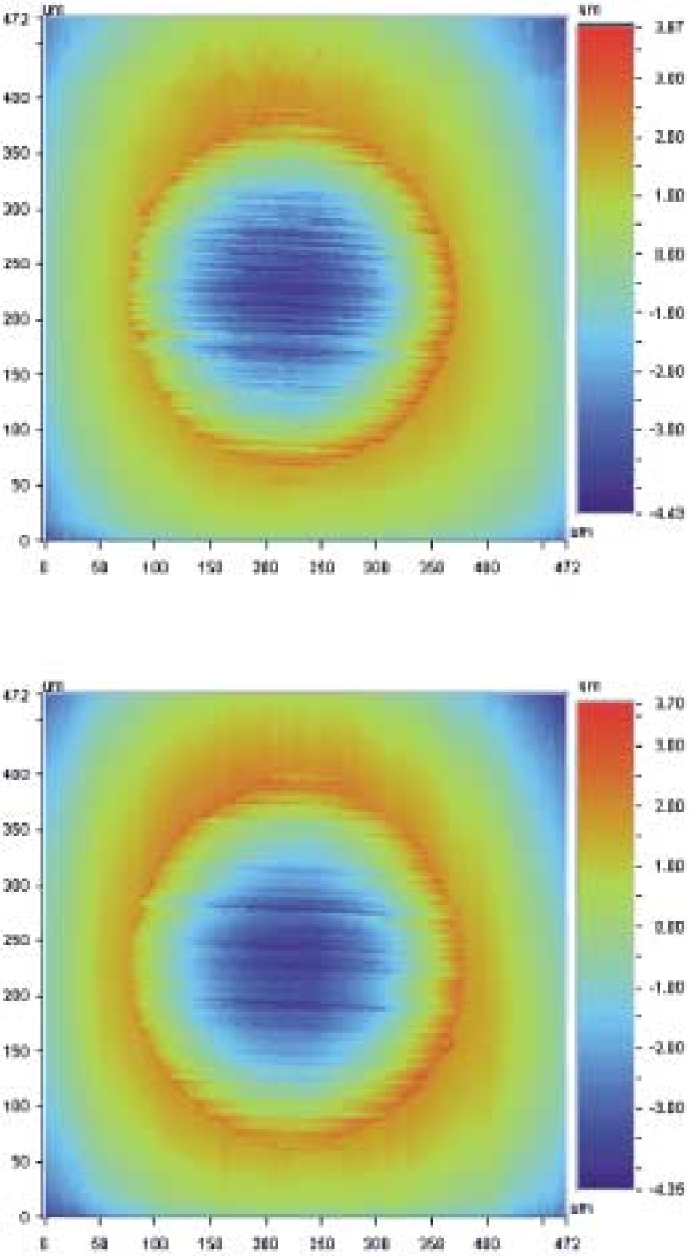

Figure 5. (a) Wear scar at 100 cycles, 1 Newton; (b) Wear scar at 10,000 cycles, 1 Newton. The scar itself is a blue region in the center of the image. Horizontal abrasion scratches are visible.

removed or lose their abrasiveness or both, at a load-dependent rate.

3.2. B_4C coating

A comparison of figure 7(a) and (b) shows how the surface morphology of the B_4C changes after 500 passes under a 52100 steel ball with a load of 1 Newton. We believe that the observed flattening of the asperities is responsible for the reduction in abrasiveness of the coating. Figure 8 compares the abrasion kinetics data for 11, 1 and 0.05 Newtons. At very low loads we see a knee similar to that observed with the Ford DLC, but at higher loads the knee disappears. (We note that figure 6 shows that the DLC data has the most prominent knee at the lowest loads). When n is large the slope for 1 and 11 Newtons is -0.78, while the slope for 0.05 Newtons is -0.94. Thus, in contrast to what we observe with the Ford DLC, the ultimate amount of material removal increases with load, and the slope never goes quite to -1, meaning that the abrasion never ceases.

When examined in more detail, the flat terraces on the B_4C seen in figure 7(b) show a nearly atomically flat

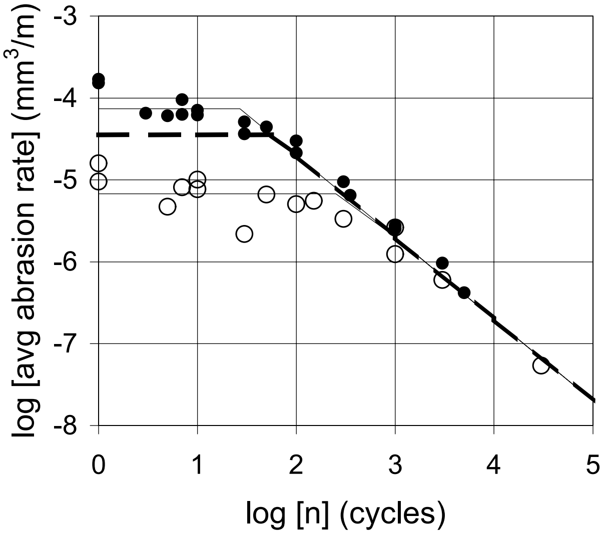

Figure 6. Abrasion kinetics for 0.02 Newton load (open circles) and 11 Newton load (solid circles) compared to 1 Newton (heavy dashed line).

surface over a region of about 0.3 × 0.3 microns, figure 7(c), with a roughness parameter below 0.4 nm. We have proposed [3] that a chemical oxidation mechanism is the most likely explanation for the smoothing of the B_4C by steel, but we cannot explain why the terraces should become so astonishingly smooth.

3.3. Comparative analysis

The abrasiveness of some sputtered carbon-containing ceramic films falls rapidly with number of cycles. We have demonstrated [6] that for a fixed load the abrasion rate is independent of the stage of wear of the steel ball and independent of the nominal average contact stress between the coupon and the ball. (This observation is most readily demonstrated by sliding a worn ball, where there is a large apparent contact area and low nominal average contact stress, against a fresh coating. The measured abrasion rate is identical to that observed using an *un*worn ball at the same load, where there is a small apparent contact area and high nominal average contact stress. This is just the result predicted from the analysis of Greenwood and Williamson [13], who showed that the number of asperities in contact depends on the load but not on the apparent contact area.) We conclude, therefore, that the reduction in abrasiveness reflects a change in the coating and is not related to changes in the ball. Instead, we correlated loss of abrasiveness with the smoothing of the nanoscale roughness of the coatings. Given the much greater roughness of the B_4C coating, we expect that it should be much more abrasive than the DLC coating, and this expectation is borne out. The initial abrasion rate of the DLC for a 1 Newton load is $A_1 = 3 \times 10^{-5}\,\text{mm}^3/\text{m}$, while that for B_4C at the same load is $A_1 = 2 \times 10^{-3}\,\text{mm}^3/\text{m}$.

We propose that the reduction in abrasiveness for a surface such as that shown for the B_4C in figure 7 occurs as follows. Initially, the entire load is carried on the highest asperities. There are perhaps half-a-dozen particularly tall asperities in figure 7(a). Assuming that this region is typical, then the areal density of such asperities is around $5 \times 10^4/\text{mm}^2$. For a contact area between the ball and the coating of 0.1 mm^2 (reached for B_4C within about 10 cycles) the steel would be supported by about 5000 of these asperities, each presenting a cross section of a few μm^2, judging from images of typical asperities (figure 7(a)). If all of these asperities participated in supporting the steel, the average contact stress at each asperity would be on the order of 50 MPa. Since this value is about 1% of the hardness of the steel ball, the load could actually be supported by just the tallest 1% of the asperities. As the tops of these highest asperities are worn down to form terraces (figure 7(b)), lower asperities are exposed to the ball. These next-generation asperities are less effective for causing further abrasion than those in the first generation because some of the load is now carried by newly-formed terraces, so fewer fresh asperities are required. Thus, the abrasion rate falls, but as long as there is a new generation of asperities to take over after a taller generation wears down, the abrasion rate remains above zero.

The case with the DLC is quite different. Because the asperity density is only around 10^1–$10^2/\text{mm}^2$, there are only a handful of asperities available to support the ball. Assuming again that each asperity presents a cross section to the steel of a few μm^2, then the available asperities can support a total of only a few hundredths of a Newton. Thus, for the 1 Newton and 11 Newton experiments, only a small fraction of the load can be carried by the asperities, with the rest supported by the flat surface of the coupon. Once the asperities lose their abrasiveness, the abrasion rate goes to zero. A load of

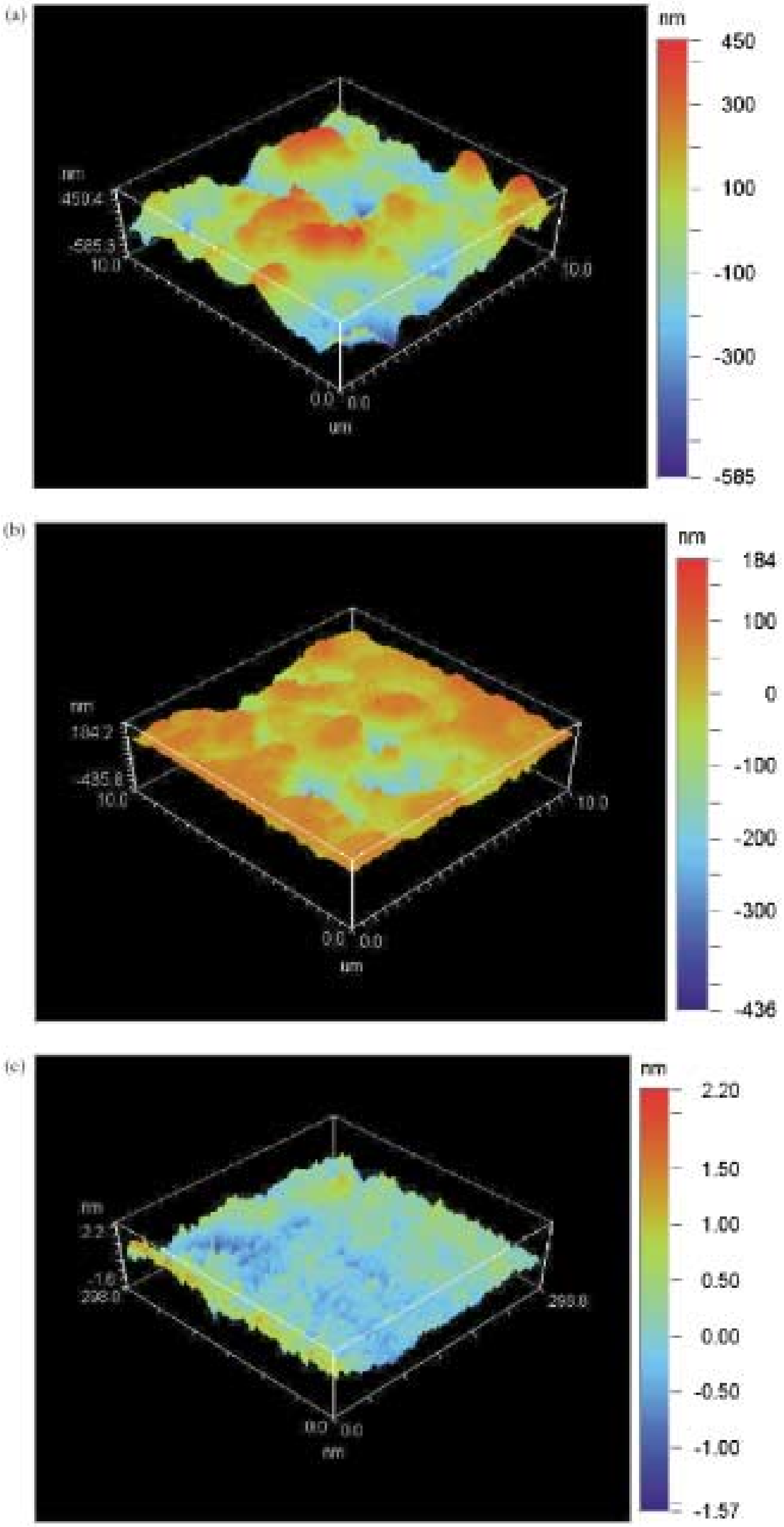

Figure 7. (a) Fresh B_4C; (b) B_4C after 500 cycles; (c) close-up AFM image of a terrace of B_4C after 500 cycles, showing a nearly atomically flat 0.3×0.3 micron region. Ra = 0.3 nm, Rq = 0.38 nm.

0.02 Newtons might be carried completely by the higher asperities, but after a few generations there are no additional asperities, and the abrasion rate again goes to zero. This picture rationalizes the observation that more cycles are required at low loads than at high loads before the abrasion rate goes to zero. The fact that the abrasiveness is constant (during the first 40–250 cycles) before going to zero suggests that there is some property of the asperities that has a threshold, above which the asperity is abrasive and below which it is not. It is known that for interfaces with low friction coefficients, low attack angles favor ploughing (with no material removal) while attack angles greater than a critical value load to cutting (with material removal) [12]. Examination of our surface profile data suggests that the critical attack angle occurs when the RMS angle on the surface is around 10°. Thus, we suggest that the polishing process reduces the attack angle of the asperities, which remain abrasive until the RMS angle drops below 10°.

4. Summary and conclusions

The fact that the B_4C remains slightly abrasive after tens of thousands of cycles while the DLC loses all its abrasiveness after a few tens or hundreds of cycles can be explained by different underlying surface morphologies. The DLC is flat—except for a few DLC particles that apparently became attached to the coating surface during the deposition—so that the abrasion rate quickly goes to zero. Future work will examine the evolution of individual asperities on the DLC and whether this evolution is mechanical or chemical. The B_4C, in contrast, is fundamentally "rough" in the sense that the columnar structure is always present no matter how much B_4C is removed. Although polishing of asperities on the tops of islands takes place, island edges as well as further asperities in the topographically depressed regions between the islands can continue to cause abrasion.

Despite the major differences in the surface topography of these two films, our results indicate that tribological interactions that polish the sharpest asperities on the harder counterface lead to extremely low abrasion rates of the softer material. If the loss of abrasiveness occurs rapidly enough, the counterpart can be polished without losing its shape or being worn away. We are now in a better position to specify an optimal surface finish for a coating. Although the production of surfaces that are smooth on the nanometer scale is generally very difficult and possibly very expensive, these results show that in some cases the task of polishing the nanometer-scale asperities can be left to the tribological system itself. This principle can be used for the selection of low-abrasion coatings.

References

[1] A. Erdemir, Surf. Coat. Technol. 54–55 (1992) 482.

[2] S.J. Harris, A.M. Weiner, C.H. Olk and M. Grischke, Wear 219 (1998) 98.

[3] S.J. Harris, G.G. Krauss, S.J. Simko, R.J. Baird, S.A. Gebremariam and G. Doll, Wear in press.

[4] S.J. Harris and A.M. Weiner, Wear 213 (1997) 200.

[5] M.A. Moore, Mater. Engin. Appl. 1 (1978) 97.

[6] S.J. Harris and A.M. Weiner, Wear 223 (1998) 31.

[7] (a) W.C. Vassell, A.K. Gangopadhyay, T.J. Potter, M.A. Tamor, and M.J. Rokosz, J. Mater. Engin. Perform. 6 (1993) 426. (b) M.W. Geis and M.A. Tamor, *Encyclopaedia of Applied Physics* Vol. 5 (VCH, New York, 1993).

[8] S.J. Harris, G. Krauss, M.T. Siniawski, Q. Wang, S. Liu and Y. Ao, Wear in press.

[9] K. Jia, Y. Li, T. Fischer and B. Ballois, J. Mater. Res. 10 (1995) 1403.

[10] K. Habig, Surf. Coat. Technol. 76–77 (1995) 534.

[11] S.J. Harris and G.G. Krauss, Tribol. Lett. 10 (2001) 187.

[12] I.M. Hutchings, *Tribology: Friction and Wear of Engineering Materials*, (CRC Press, Ann Arbor, 1992), ch. 6.

[13] J.A. Greenwood and J.B.P. Williamson, Proc. Roy. Soc. Lond. A295 (1966) 300.